Pr-magnetism in the quasi-skutterudite compound PrFe$_2$Al$_8$

Pr-magnetism in the quasi-skutterudite compound PrFe$_2$Al$_8$

Harikrishnan S. Nair[1,2], Michael O. Ogunbunmi[1], C. M. N. Kumar[3], D. T. Adroja[4,1], P. Manuel[4], D. Fortes[4], J. Taylor[4], A. M. Strydom[1]

[1]Highly Correlated Matter Research Group, Physics Department, P. O. Box 524, University of Johannesburg, Auckland Park 2006, South Africa

[2]Department of Physics, Colorado State University, 200 W. Lake St., Fort Collins, CO 80523-1875, USA

[3]Laboratoire National des Champs Magnétiques Intenses, CNRS-INSA-UJF-UPS, 143 Avenue de Rangueil, F-31400 Toulouse, France

[4]ISIS Facility, STFC, Rutherford Appleton Laboratory, Chilton, Didcot, Oxfordshire OX11 0QX, United Kingdom

E-mail: `h.nair.kris@gmail.com`, `hsnair@colostate.edu`

Pr-magnetism $PrFe_2Al_8$ 2

Abstract. The intermetallic compound $PrFe_2Al_8$ that possesses a three-dimensional network structure of Al polyhedra centered at the transition metal element Fe and the rare earth Pr is investigated through neutron powder diffraction and inelastic neutron scattering in order to elucidate the magnetic ground state of Pr and Fe and the crystal field effects of Pr. Our neutron diffraction study confirms long-range magnetic order of Pr below $T_N = 4.5$ K in this compound. Subsequent magnetic structure estimation reveals a magnetic propagation vector $\mathbf{k} = (\frac{1}{2}\ \mathbf{0}\ \frac{1}{2})$ with a magnetic moment value of 2.5 μ_B/Pr along the orthorhombic c-axis and evidence the lack of ordering in the Fe sublattice. The inelastic neutron scattering study reveals one crystalline electric field excitation near 19 meV at 5 K in $PrFe_2Al_8$. The energy-integrated intensity of the 19 meV excitation as a function of $|Q|(\mathring{A}^{-1})$ follows the square of the magnetic form factor of Pr^{3+} thereby confirming that the inelastic excitation belongs to the Pr sublattice. The second sum rule applied to the dynamic structure factor indicates only 1.6(2) μ_B evolving at the 19 meV peak compared to the 3.58 μ_B for free Pr^{3+}, indicating that the crystal field ground state is magnetic and the missing moment is associated with the resolution limited quasi-elastic line. The magnetic order occurring in Pr in $PrFe_2Al_8$ is counter-intuitive to the symmetry-allowed crystal field level scheme, hence, is suggestive of exchange-mediated mechanisms of ordering stemming from the magnetic ground state of the crystal field levels.

Pr-magnetism $PrFe_2Al_8$ 3

1. Introduction

Intermetallic compounds possessing a cage-like crystal structure comprising of polyhedra that contain rare earth or transition metal atoms in their voids have been interesting compounds from the perspective of thermoelectric properties, however, the magnetism of rare earth that is placed in the cages is a relatively less-explored topic. The filled-skutterudites RT_4X_{12} where R = rare earth, T = transition metal and X = pnictogen, is a well-explored class of compounds [1, 2] with the potential of making thermoelectric applications [3]. The original binary skutterudite formula can be written as TX_3 which, with the existence of voids in the original $Im3$ structure, may adopt a general formula $R_2M_8X_{24}$ or RM_4X_{12}. The cubic RT_2Al_{20}, known as the Frank Kasper compounds, provide another example of the caged-structure compounds similar to the filled-skutterudites, and have a large coordination number of atoms constructing the cage around the R atom[4]. They crystallize in the space group $Fd\bar{3}m$ (#227) with the R ion surrounded by neighboring 16 atoms and the R site is of a cubic point symmetry. A related caged-structure compound is the RT_2Al_{10} which has orthorhombic crystal structure with the space group $Cmcm$ (#63) [5, 6]. In this caged system the R atoms are 20-fold coordinated and are located inside $T-$Al cages. It is interesting to look at the magnetism of these caged-network compounds with Pr occupying the void inside the cage. For example, the filled-skutterudite $PrRu_4Sb_{12}$ shows a Van Vleck paramagnetic behaviour for most of the temperature range before entering a superconducting phase below 1.04 K[7, 8]. In the case of $PrTi_2Al_{20}$, a non-magnetic order parameter was identified below the magnetic transition at 2 K[9]. This was correlated with the ferroquadrupole ordering scenario. In the case of $PrRu_2Al_{10}$, which displayed metallic behaviour, no magnetic phase transition was recorded down to low temperature[10]. These studies focusing on the rare earth magnetism in the caged-network points towards the interesting magnetic ordering or the lack of it, that may have a strong influence from the ligand field around the rare earth. The crystal field ground state of the $4f$ ion in the cages play an important role in the magnetic ordering phenomena in these compounds. While many studies focused on the magnetism of the $4f$ element in the cages, it must be noted that the magnetism of the $3d$ element and the correlation between the two is an emergent theme in similar compounds. For example, *ab-initio* calculations in the $Ce_3T_4X_{13}$ compounds have shown indication of correlation between the $3d$ and the $4f$ wave functions[11]. Unexpected localization of Fe $3d$ moments were experimentally observed in another caged compound $Yb_2Fe_2Al_{10}$ where it was observed that the long-range ordering of the $3d$ moments were avoided down to 0.4 K[12]. These studies point to case of caged intermetallics where the rare earth and transition metal display cooperative phenomena in concert or as separate. With this background, we take a look at a rather less-studied caged-network intermetallic compound, $PrFe_2Al_8$ that belongs to the family of RT_2X_8 (X = Al, Ga).

The RT_2X_8 compounds crystallize in cubic $Pbam$ space group. Figure 1 shows the projection of the crystal structure on *ab*-plane displaying the network of Al and

Pr-magnetism PrFe$_2$Al$_8$ 4

the chain-like formation of Pr and Fe along the c-axis. These structural peculiarities certainly have a bearing on the magnetism of this class of compounds, notably, a strong influence from crystal field effects. Depending on whether the crystal field levels are comparable in energy scales with other interactions (especially, magnetic exchange), a non-magnetic singlet or doublet crystal field ground state can result. To cite an example, the point charge model calculations that take in to account the local symmetry for the Pr site in PrSi predicts a splitting of $J = 4$ Pr^{3+} ground state in to 9 singlets which renders spontaneous magnetic order impossible. However, an anomalous ferromagnetic ground state (with an ordering temperature of ≈ 55 K) was experimentally unraveled in PrSi[13]. Similarly, the point symmetry of the Pr-site in PrFe$_2$Al$_8$ is m (C_s) which predicts 9 distinct singlets from a 9-fold degenerate state which consequentially presupposes a non-magnetic ground state. Our previous studies on PrFe$_2$Al$_8$ had revealed long-range magnetic order through macroscopic magnetization measurements which was assumed to have originated from the Pr magnetic sublattice[14]. The Fe sublattice was deduced to be non-magnetic or as having only short-range spin correlations. In the present work, we investigate the magnetic ground state of PrFe$_2$Al$_8$ through neutron diffraction experiments and confirm that only Pr orders magnetically long-range while Fe is not. In addition, our study sheds light on the magnetic excitations and crystal field effects through inelastic neutron scattering.

2. Experimental details

About 10 g of polycrystalline powder of PrFe$_2$Al$_8$ and LaFe$_2$Al$_8$ were prepared following the procedure outlined in Ref.[14]. The powder samples were initially characterized using laboratory x-rays to check for purity of the chemical phase and using magnetometry to identify the magnetic phase transition. These preliminary checks confirmed the findings of Ref.[14]. Time-of-flight (TOF) neutron powder diffraction experiments were carried out at the instrument HRPD at ISIS facility of the Rutherford Appleton Laboratory, UK mainly to characterize the temperature evolution of the crystal structure. Diffraction patterns covering a d-spacing range 0.75 - 4 Å were obtained at 19 temperature points in the interval of 300 K to 1.6 K. Additionally, experiments were also performed using the TOF diffractometer WISH on TS2 at ISIS facility especially covering the higher d-spacing range of 1.2 - 11 Å in order to unambiguously determine the magnetic structure of PrFe$_2$Al$_8$. Inelastic neutron scattering experiments were performed on 10 g of PrFe$_2$Al$_8$ powder sample using the TOF chopper spectrometer MARI at ISIS facility. PrFe$_2$Al$_8$ powder from the same batch was used in all the three experiments. Incident neutron energies $E_i = 8$ meV, 50 meV and 150 meV were selected for the experiment. The chopper frequencies were set at 150 Hz, 250 Hz, and 400 Hz, respectively. Data were collected mainly at 5 K, 50 K, 200 K and at 300 K. As a non-magnetic reference, the inelastic response of LaFe$_2$Al$_8$ was also recorded to serve as a phonon estimate for PrFe$_2$Al$_8$. The inelastic neutron data was analyzed using the software DAVE[15]. Rietveld refinement[16] of the diffraction data were carried out using FULLPROF

Pr-magnetism PrFe$_2$Al$_8$ 5

software [17]. The software SARAh[18] was used for the representation analysis of magnetic structure from diffraction data.

3. Results

3.1. Neutron Diffraction

A 2D contour plot of the diffracted intensity from PrFe$_2$Al$_8$ obtained from the diffraction data of bank-3 of HRPD, is shown in figure 2 as a function of temperature and d-spacing. Diffracted intensity due to Bragg scattering from the nuclear structure is present at $d \approx$ 4 Å, 5.5 Å, 6.2 Å, 7.2 Å and 9.5 Å. It is observed that additional magnetic intensity develops only below 4 K, at the d-spacing 5.3 Å, which is indicated in figure 2 by a horizontal white dashed-line. Note that the temperature-axis is plotted in log-scale for clarity. According to our previous investigation on PrFe$_2$Al$_8$ [14], long-range magnetic order sets in only below $T_N^{Pr} \approx 4$ K. The experimental evidence in figure 2 supports this assignment of magnetic phase transition temperature $T_N^{Pr} \approx 4$ K for Pr. In our previous work signatures akin to short-range spin fluctuations in the Fe lattice were observed in magnetic susceptibility at $T_{anom} \approx 34$ K. No magnetic scattered intensity is developed at around 34 K in the present diffraction data thereby ruling out the presence of magnetic ordering on the Fe lattice in this compound. More concretely, in a later subsection of the present paper, it is shown through inelastic neutron data that the energy-integrated intensity as a function of $|Q|$ follows the magnetic form factor of Pr^{3+} there by confirming that only Pr orders magnetically in PrFe$_2$Al$_8$.

The neutron powder diffraction intensity pattern of PrFe$_2$Al$_8$ at 25 K obtained from HRPD, is plotted in figure 3 (a) (black circles) as a function of d-spacing. The red solid line in the figure is the result of a Rietveld fit to the data using *Pbam* space group. From the magnetization measurements we know that at 25 K PrFe$_2$Al$_8$ is not magnetically ordered and hence the diffraction data was modeled using only the nuclear structure in the space group model *Pbam* as has been used in our previous work [14]. The diffracted intensity at 300 K (not shown) is similar to that at 25 K as presented in figure 3 (a) and no signature of any structural phase transition is observed in this temperature interval of 300 - 25 K. The lattice parameters a, b and c show a gradual decrease with temperature as can be seen from the values at 300 K, 150 K and 25 K collected in Table (1). Also presented in Table (1) are the atomic parameters of PrFe$_2$Al$_8$ at 300 K. The crystal structure of PrFe$_2$Al$_8$ in *Pbam* space group has Pr occupying a single Wyckoff position $4g$[19]. The crystal structure is a close-packed arrangement of three dimensional Al polyhedra which are packed face-sharing to form chains of Pr and Fe along the c-axis separated from each other by the Fe-Al network (see figure 1). The shortest Pr-Pr and Fe-Fe distances are parallel to the c-axis. As a function of temperature, the Pr-Pr and the Fe-Fe nearest-neighbour distances undergo only slight variation. A slight decrease in the nearest-neighbour distances is observed in all the directions a, b and c. The bond angles between the nearest Pr atoms also do not vary significantly down till 1.6 K. Along

Pr-magnetism PrFe$_2$Al$_8$ 6

a and b directions, they remain close to the values 144° and 145° respectively. The bond parameters as a function of temperature are collected in Table (2).

One of the important questions about the magnetism of PrFe$_2$Al$_8$ is whether Pr and Fe in this compound order in a magnetically long-range fashion, either individually or jointly, or not. In our previous study[14], magnetic anomalies at $T_{anom} \approx 34$ K and $T_N^{\mathrm{Pr}} \approx 4$ K were observed in the magnetization measurements. The anomaly at T_{anom} was attributed to short-range order in the Fe lattice or due to minute amount of magnetic impurity; whereas T_N^{Pr} was attributed to long-range order in the Pr magnetic lattice. Hence, one of the major aims of our neutron diffraction experiments was to determine the microscopic nature of the magnetic phase transitions pertaining to Fe or Pr in PrFe$_2$Al$_8$. Since, through the low angle bank of HRPD, the development of long-range magnetic order in the Pr sublattice was observed to occur below 4 K, we performed a detailed low temperature neutron diffraction measurements using the WISH diffractometer in the temperature range 2 K to 50 K covering a larger d-spacing up to 11 Å. The diffracted intensity at 50 K was identical to that of 20 K. No additional magnetic Bragg peaks or short range magnetic diffuse scattering were observed at 20 K. Also, there was no enhancement of diffracted intensity at low temperatures suggesting ferromagnetic contributions at nuclear Bragg positions. These results confirm that the 34 K transition observed previously[14] in the magnetic susceptibility is not from the bulk of the sample.

The neutron diffraction patterns at 20 K and 2 K obtained from WISH along with the Rietveld refinement results are presented in figure 3 (b), (c) and (d). It can be readily observed that additional scattered intensity has developed at 2 K as compared to the intensity profiles at high temperatures. Especially, new peaks at $d \approx 5.25$ Å, 5.37 Å, 6.78 Å and 7.68 Å emerge. The nuclear structure below $T_N^{Pr} \approx 4$ K conforms to *Pbam*, which is the crystal structure at 300 K. Hence, any structural phase transformation in the temperature range 300 - 4 K is ruled out. In order to ascertain the ordering is from Pr or Fe or from both in PrFe$_2$Al$_8$ first, a determination of the magnetic propagation vector was undertaken. Using the k-search utility in the FULLPROF suite of programs, the most probable propagation vector was determined as $\mathbf{k}(\frac{1}{2}\ \mathbf{0}\ \frac{1}{2})$ to be used for the representation analysis of magnetic structure. According to the symmetry analysis for the orthorhombic *Pbam* space group, two magnetic representations Γ_1 and Γ_2 - both antiferromagnetic - were found as acceptable solutions for the magnetic structure of Pr^{3+} in PrFe$_2$Al$_8$. Hence, Rietveld refinement of diffracted intensity at 2 K was performed by assuming the nuclear space group as *Pbam* and the magnetic representation as Γ_1 or Γ_2. The magnetic R-factor for the refinements with Γ_1 or Γ_2 were 3.4 and 80 respectively, indicating that Γ_1 is the best fit. In this representation, Pr moments order antiferromagnetically with moment direction along the orthorhombic c-axis. In the panel (d) of Figure 3, the Rietveld refinement of 2 K data of PrFe$_2$Al$_8$ is shown, with the fits using Γ_2 representation (lower tick marks). Noticeably, the intensities are not correctly accounted for in this model (near $d \approx 5.5$ Å and 7.7 Å). A refinement model that allows for long-range magnetic order in both Pr and Fe lattices did not lead to an improved fit

Pr-magnetism PrFe$_2$Al$_8$ 7

and hence was discarded. The experimental data did not fit to a model that considers only the Fe moment ordering, either. Moreover, from our previous experimental study[14] it was understood that the magnetic anomaly tentatively attributed to Fe at T_{anom} was very broad suggesting short-range correlations to be present rather than a conventional paramagnet-to-antiferromagnet phase transition. A value of 2.5 μ_{B}/Pr is obtained at 2 K for the neutron-derived ordered moment of Pr. A gradual decrease of the ordered magnetic moment was observed until $T_N^{Pr} = 4.5$ K. The temperature-evolution of the ordered moment of Pr, M_{Pr}, is presented in the inset of figure 3 (c). The dashed line in the inset serves as a guide to eye. The antiferromagnetic Γ_1 magnetic structure adopted by Pr^{3+} moments in PrFe$_2$Al$_8$ is pictured in figure 4.

3.2. Inelastic Neutron Scattering

Once we determined the magnetic structure of PrFe$_2$Al$_8$ we now proceed to study the magnetic excitations and the crystal field effects using inelastic neutron scattering methods. The inelastic neutron scattering intensity of PrFe$_2$Al$_8$ at different incident neutron energies and temperatures are presented in figure 5 (a) through (f) where color maps of energy transfer (in meV) versus momentum transfer ($|Q|$ in $\mathring{A}^{-1}$) are shown. Specifically, (a) $E_i = 8$ meV, $T = 5$ K, (b) $E_i = 50$ meV, $T = 5$ K and (c) $E_i = 50$ meV, $T = 200$ K for PrFe$_2$Al$_8$ are shown. The inelastic intensity of the non-magnetic reference compound LaFe$_2$Al$_8$ are shown in (d) $E_i = 8$ meV, $T = 5$ K, (e) $E_i = 50$ meV, $T = 5$ K and (f) $E_i = 50$ meV, $T = 200$ K. The intensity pattern at 5 K and at 200 K are essentially identical, suggesting that there is no magnetic low lying excitations in the energy range approximatley up to 10 meV. The absence of any excited state transition at 200 K suggests that there are no CEF levels below 15 meV, which have non-zero matrix elements. At low energy transfer, for example with $E_i = 8$ meV (shown in (a)), no magnetic inelastic excitations are observed in PrFe$_2$Al$_8$. This result indicates that the quasi-elastic linewidth is very small and not able to detect within the resolution of MARI ($\Delta E = 0.19$ meV for $E_i = 8$ meV, 150 Hz). In figure 5, only one inelastic excitation is seen present at all the temperatures, *viz.,* at 19 meV which arises from the crystal field excitation of the Pr^{3+} crystal field levels, as can be seen from the panel (b) with incoming energy, $E_i = 50$ meV at 5 K. The inelastic spectra shown in figure 5 also suggest the absence of magnetic ordering down to 5 K, as one would expect spin wave excitations in an ordered state. Further the $|Q|$-dependent cuts (not shown) obtained by binning the energy from -2 meV to 2 meV (from (a) and (b)) did not reveal any magnetic Bragg peaks at 5 K. From panels (d, e) that represent the inelastic scattered intensity of LaFe$_2$Al$_8$ at 5 K, it is clear that no magnetic intensity is present in the non-magnetic analogue compound, which indicates that the Fe atoms do not have ordered magnetic moments in LaFe$_2$Al$_8$ or PrFe$_2$Al$_8$. An E versus $|Q|$ plot of PrFe$_2$Al$_8$ obtained using $E_i = 150$ meV (not shown here) also did not provide any evidence of other CEF excitations between 20 meV and 145 meV. The high intensity observed in (d) towards the high-Q originates from the phonon contribution. The inelastic intensity of PrFe$_2$Al$_8$

Pr-magnetism PrFe₂Al₈　　　　　　　　　　　　　　　　　　　　　　　　8

at 200 K (in (c)) is compared with that of $LaFe_2Al_8$ in the panels (e) and (f), which further confirmed that high-$|Q|$ intensity is mainly dominated by the phonon scattering as its intensity shows an increase with increasing temperature.

The $|Q|$-integrated (0 to 3 $\mathring{A}^{-1}$) dynamic structure factor, $S(Q,\omega)$, for $PrFe_2Al_8$ as a function of energy transfer at $E_i = 50$ meV is presented in figure 6 (a) for 5 K, 50 K and 200 K. The location in the graph where energy transfer equals zero corresponds to the elastic line. The inelastic signal arising from the crystal field effect is observed at 19 meV which diminishes in intensity as temperature is raised. The $S(Q,\omega)$ dependence on energy transfer with $E_i = 8$ meV is shown in the inset (a1), which shows the absence of any excitations in the energy range accessed. The dynamic structure factor for inelastic neutron scattering of unpolarized neutrons is given by the equation[20],

$$S(Q,\omega) = \frac{\hbar\omega}{1-\exp(-\hbar\omega/k_BT)}F^2(Q)\chi_0 P(Q,\hbar\omega) \tag{1}$$

where $F(Q)$ is the magnetic form factor of the magnetic ion, χ_0 is the static magnetic susceptibility and $P(Q,\hbar\omega)$ is a spectral function. The first term on the right-hand-side is the Bose factor for the thermal occupation of levels. Curve fits to the 19 meV excitation according to Equation (1) is shown in Figure 6 (b) for 5 K, 50 K and 200 K. The FWHM of the peaks as well as the area under the peak which corresponds to the local susceptibility were extracted from these fits and presented respectively in panels (c) and (d) of Figure 6. A gradual broadening of the peaks with increasing temperature is observed, suggested by the increasing FWHM and decreasing susceptibility. A peak is observed at $E \approx 12$ meV for the 200 K data (in the main panel of (a)) which, in fact, is narrower than the resolution and hence is judged as a spurious peak. The $|Q|$-dependence of integrated intensity at 5 K, binned in the interval of 19 - 21 meV is shown in the panel (e) plotted together with the square of the magnetic form factor, $F^2(Q)$ for Pr^{3+}. The integrated intensity follows the $F^2(Q)$ for Pr^{3+} closely, suggesting that the inelastic excitation in $PrFe_2Al_8$ results from single ion effects of Pr^{3+}. In order to estimate the magnetic moment from the inelastic signal at 19 meV, use was made of the second sum rule:

$$\int_{-\omega}^{\omega} S(Q,\omega)/F^2(Q)d\omega = A\mu_{eff}^2 \tag{2}$$

where $S(Q,\omega)$ is the dynamic structure factor, $F(Q)$ is the magnetic form factor, $A = 48.6$ mb/sr/μ_B^2 is a constant[20] and μ_{eff} is the effective magnetic moment. From the integrated intensity at the 19 meV peak of $PrFe_2Al_8$ the effective moment value was estimated as $\mu_{eff} = 1.6(2)$ μ_B which is almost half of the spin-orbit coupled magnetic moment $\mu_{so}^{Pr} = 3.58$ μ_B of Pr^{3+}, $J = 4$. The low value of the moment associated with 19 meV excitation along with the heat capacity results, which suggest a doublet CEF ground state, indicates that the missing Pr moment is associated with a narrow resolution limited quasi-elastic scattering from the ground state.

4. Discussion

The specific heat of PrFe$_2$Al$_8$ showed a clear indication of a peak at $T_N^{\mathrm{Pr}} \approx 4$ K where the Pr begins to order magnetically[14]. The magnetic contribution to the specific heat was obtained by subtracting the non-magnetic specific heat of LaFe$_2$Al$_8$. The estimate of crystal field levels were obtained by modeling the Schottky peak using a 9-level model for the crystal field levels. The first excited crystal field level was calculated at ≈ 10 K and from the behaviour of magnetic entropy as a function of temperature, a full occupation of the 9 levels was found to happen at ≈ 200 K where the entropy reaches $R \ln(9)$. From the inelastic neutron scattering data, a single excitation is discernible at 19 meV which corresponds to ≈ 200 K. The first excited level near 10 K (≈ 0.8 meV) is not observed in the inelastic data with either $E_i = 8$ meV or 50 meV, which could be due to the zero matrix element between these wave functions - the intensity of CEF excitation vary as a square of this matrix element. However, since only one excitation is revealed in the inelastic scattering experiment, a full crystal field analysis to estimate all the 9 crystal field levels is not possible in the present case. Considering orthorhombic point symmetry (C_s) of Pr ion in PrFe$_2$Al$_8$ there will be nine non-zero crystal field parameters in the Hamiltonian and hence a single observed CEF excitation is not sufficient to fit the CEF model. The temperature dependence of the inelastic excitation peak at 19 meV shown in figure 6 (a) indicates that the peak position does not shift with temperature, confirming the origin of the excitation to be crystal field effect. Moreover, the integrated intensity at 19 meV as a function of Q follows the square of form factor $F^2(Q)$ of Pr^{3+} confirming that the magnetism in PrFe$_2$Al$_8$ is purely from Pr^{3+}. Though the previous magnetization study of PrFe$_2$Al$_8$ indicated short-range magnetic order due to Fe, the neutron scattering results (figure 2) do not show any indication of this. The diffraction results only indicate that the long-range magnetic ordering in PrFe$_2$Al$_8$ at 4.5 K pertains only to the Pr sublattice where the moments order antiferromagnetically. The crystal field level scheme for $J = 4$, Pr^{3+} in the local symmetry of m predicts a singlet ground state. The $2J + 1 = 9$ fold multiplet of Pr^{3+} splits so that a crystal field singlet is always present for all type of crystallographic symmetry[21]. Pr-based intermetallics often display singlet ground states however, also have been found to lead to exotic behaviour such as the observation of heavy fermion superconductivity[22, 23]. Not only that, in certain Pr based systems like PrAu$_2$Si$_2$-related compounds, frustration effects on the magnetic ground state were argued to be introduced by crystal field effects[24]. In fact, a competition between the crystal field interaction and the magnetic exchange energy strengths were observed in these compounds, eventually, resulting in a novel spin glass ground state. Magnetic long range order also happens in several systems despite the crystal field level scheme warranting otherwise. PrIrSi$_3$ is one such system where Pr displays long range magnetic order[25]. However a large separation of about 90 K is observed between the first excited crystal field levels of PrIrSi$_3$. Induced moment magnetic ordering in this compound would require very high internal exchange energy to achieve ordering. In some other Pr-based compounds like PrRu$_2$Si$_2$ and PrNi$_2$Si$_2$,

Pr-magnetism PrFe$_2$Al$_8$ 10

relatively smaller crystal field separations are (of 2.25 meV and 3.3 meV, respectively) [26, 27]. In the present case of PrFe$_2$Al$_8$ the knowledge of the first excited crystal field level first originated from a simulation of the Schottky specific heat, which predicts the first level at around 10 K. An estimation of the exchange constant is in general possible through the relation, $\theta_p = \left[\frac{J_{\mathrm{ex}}J(J+1)}{3k_{\mathrm{B}}}\right]$ where θ_p is the Curie-Weiss temperature and J_{ex} is the exchange constant. However, in the case of PrFe$_2$Al$_8$ it was found that the inverse magnetic susceptibility did not follow a linear trend due to the presence of Fe short-range fluctuations and hence a mean-field estimate of θ_p was not possible. Comparing the ground state energy scale in PrFe$_2$Al$_8$ with other compounds like PrIrSi$_3$ or with PrRu$_2$Si$_2$ and PrNi$_2$Si$_2$, it seems more plausible that an exchange-generated admixture of low lying crystal field energy levels is possible in the case of PrFe$_2$Al$_8$.

5. Conclusions

In conclusion, through neutron powder diffraction and inelastic scattering experiments we determined the magnetism of the quasi-skutterudite compound PrFe$_2$Al$_8$.Through the analysis of the neutron diffraction data, it is found that only Pr develops long-range magnetic order in this compound with a $T_N^{\mathrm{Pr}} = 4.5$ K. The Pr^{3+} moments adopt antiferromagnetic arrangement with moments along the c-axis and a propagation vector **k**$(\frac{1}{2}$ **0** $\frac{1}{2})$. Only one magnetic excitation at 19 meV is observed in the inelastic neutron scattering data of PrFe$_2$Al$_8$ corresponding to the crystal field excitation from Pr^{3+} levels. The presence of only one excitation detected in our experiments has rendered the estimation of the full crystal field level scheme of Pr^{3+} in PrFe$_2$Al$_8$ impossible as there are nine free crystal field parameters to be determined from the one excitation. However, from the $|Q|$-dependence of integrated magnetic intensity it is confirmed that the magnetism in PrFe$_2$Al$_8$ is solely governed by Pr while the Fe sublattice remains magnetically inactive down to 2 K.

Acknowledgements

References

[1] Sales B C, Mandrus D and Williams R K 1996 *Science* **272** 1325
[2] Nolas G S, Morelli D T and Tritt T M 1999 *Ann. Rev. Mater. Sci.* **29** 89–116
[3] Guo J Q, Geng H Y, Ochi T, Suzuki S, Kikuchi M, Yamaguchi Y and Ito S 2012 *J. Elec. Mater.* **41** 1036–1042
[4] Frank F C and Kasper J S 1958 *Acta Crystallogr.* **11** 184–190
[5] Tursina A I, Nesterenko S N, Murashova E V, Chernyshev I V, Nol H and Seropegin Y D 2005 *Acta Crystallogr. E* **61** i12–i14

Pr-magnetism PrFe$_2$Al$_8$ 11

[6] Adroja D T, Hillier A D, Muro Y, Takabatake T, Strydom A M, Bhattacharyya A, Daoud-Aladin A and Taylor J W 2013 *Physica Scripta* **88** 068505

[7] Takeda N and Ishikawa M 2000 *J. Phys. Soc. Jpn.* **69** 868–873

[8] Adroja D T, Hillier A D, Park J G, Goremychkin E A, McEwen K A, Takeda N, Osborn R, Rainford B D and Ibberson R M 2005 *Physical Review B* **72** 184503

[9] Ito T U, Wataru H, Kazuhiko N, Hubertus L, Christopher B, Akito S and Satoru N 2011 *J. Phys. Soc. Jpn.* **80** 113703

[10] Masahito S, Kazuhiro K, Shuhei T, Eiichi M, Hitoshi S, Matsuda T D and Yoshinori H 2012 *J. Phys. Soc. Jpn.* **81** SB011

[11] Ślebarski A, Goraus J, Witas P, Kalinowski L and Fijałkowski M 2015 *Phys. Rev. B* **91** 035101

[12] Khuntia P, Peratheepan P, Strydom A M, Utsumi Y, Ko K T, Tsuei K D, Tjeng L H, Steglich F and Baenitz M 2014 *Phys. Rev. Lett.* **113** 216403

[13] Snyman J L and Strydom A M 2012 *J. Appl. Phys.* **111** 07A943

[14] Nair H S, Ghosh S K, Rameshkumar K and Strydom A M 2016 *J. Phys. Chem. Solids* **91** 69–75

[15] Azuah R T, Kneller L R, Qiu Y, Tregenna-Piggott P L W, Brown C M, Copley J R D and Dimeo R M 2009 *J. Res. Nat. Inst. Standards and Tech.* **114** 341

[16] Rietveld H M 1969 *J. Appl. Crystall.* **2** 65–71

[17] Rodriguez-Carvajal J 2010 *LLB, CEA-CNRS, France [http://www. ill. eu/sites/fullprof/]*

[18] Wills A S 2000 *Physica B* **276** 680–681

[19] Tougait O, Kaczorowski D and Noël H 2005 *J. Solid State Chem.* **178** 3639–3647

[20] Holland-Moritz E, Wohlleben D and Loewenhaupt M 1982 *Phys. Rev. B* **25** 7482

[21] Walter U 1984 *J. Phys. Chem. Solids* **45** 401–408

[22] Bauer E D, Frederick N A, Ho P C, Zapf V S and Maple M B 2002 *Phys. Rev. B* **65** 100506

[23] E A Goremychkin, Osborn R, Bauer E D, Maple M B, Frederick N A, Yuhasz W M, Woodward F M and Lynn J W 2004 *Phys. Rev. Lett.* **93** 157003

[24] Goremychkin E A, Osborn R, Rainford B D, Macaluso R T, Adroja D T and Koza M 2008 *Nat. Phys.* **4** 766–770

[25] Anand V K, Adroja D T, Bhattacharyya A, Hillier A D, Taylor J W and Strydom A M 2014 *J. Phys.: Condens. Matter* **26** 306001

[26] A M Mulders, Yaouanc A, Dalmas de Rotier P, Gubbens P C M, Moolenaar A A, Fk B, Ressouche E, Proke K, Menovsky A A and Buschow K H J 1997 *Phys. Rev. B* **56** 8752–8759

[27] Blanco J A, Gignoux D and Schmitt D 1992 *Phys. Rev. B* **45** 2529–2532

Pr-magnetism PrFe$_2$Al$_8$

12

Table 1. The lattice parameters of PrFe$_2$Al$_8$ obtained from the refinement of neutron diffraction data at 300, 150 and 25 K are provided in the top section of the table. The refined atomic coordinates of PrFe$_2$Al$_8$ at 300 K are given in the bottom section. These values are obtained from the HRPD-data.

		300 K	150 K	25 K	
a (Å)		12.5101(3)	12.4871(5)	12.4799(4)	
b (Å)		14.4383(3)	14.4168(6)	14.4081(8)	
c (Å)		4.0411(1)	4.0332(8)	4.0297(2)	
PrFe$_2$Al$_8$, *Pbam*, 300 K					
Atom	site	x	y	z	U_{iso}
Pr	$4g$	0.34430	0.31793	0.0	0.0029
Fe(1)	$4g$	0.15095	0.09235	0.0	0.0018
Fe(2)	$4g$	0.03619	0.40434	0.0	0.0021
Al(1)	$2d$	0.0000	0.5000	0.5	0.0033
Al(2)	$2a$	0.0000	0.0000	0.0	0.0053
Al(3)	$4h$	0.02968	0.13355	0.5	0.0053
Al(4)	$4h$	0.16160	0.3761	0.5	0.0031
Al(5)	$4h$	0.23677	0.17102	0.5	0.0035
Al(6)	$4h$	0.33260	0.49029	0.5	0.0034
Al(7)	$4h$	0.45987	0.18346	0.5	0.0028
Al(8)	$4g$	0.33473	0.03719	0.0	0.0041
Al(9)	$4g$	0.09153	0.25152	0.0	0.0043

Pr-magnetism PrFe$_2$Al$_8$ 13

Table 2. The Pr-Pr and the Fe-Fe nearest-neighbour distances and angles of PrFe$_2$Al$_8$ at 300 K, 150 K, 25 K and 1.6 K. The distances along a, b and c directions are shown. The angle shown is that which is formed between any three nearest-neighbour Pr atoms.

	300 K	150 K	25 K	1.6 K
Pr-Pr ($\parallel c$)	4.0411(9) Å	4.0334(6) Å	4.0297(2) Å	4.0297(2) Å
Pr-Pr ($\parallel a$)	6.572(9) Å	6.562(11) Å	6.559(11) Å	6.554(13) Å
Pr-Pr ($\parallel b$)	7.563(7) Å	7.554(7) Å	7.551(9) Å	7.560(9) Å
Fe-Fe ($\parallel c$)	4.0411(2) Å	4.0335(6) Å	4.0297(6) Å	4.0297(8) Å
Fe-Fe ($\parallel a$)	4.818(14) Å	4.815(4) Å	4.816(5) Å	4.817(6) Å
Fe-Fe ($\parallel b$)	2.754(4) Å	2.748(5) Å	2.757(5) Å	2.762(7) Å
$\angle$ Pr ($\parallel a$)	144.23(8)°	144.12(7)°	144.12(7)°	144.36(9)°
$\angle$ Pr ($\parallel b$)	145.32(9)°	145.19(11)°	145.15(10)°	145.68(11)°

Pr-magnetism PrFe$_2$Al$_8$ 14
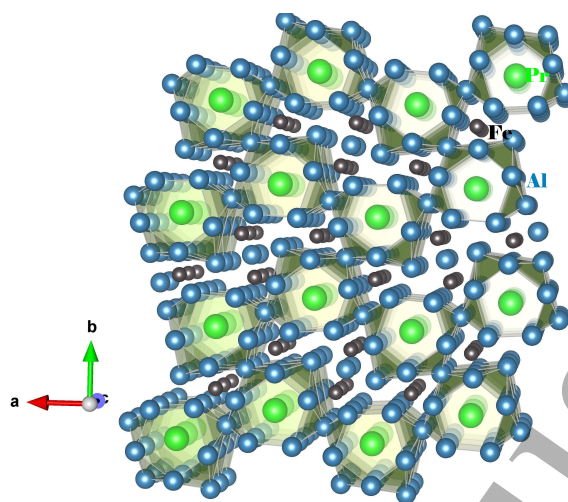
Figure 1. (color online) A schematic representation of the cage-like network structure of the quasi-skutterudite PrFe$_2$Al$_8$. A projection of the cages on the *ab* plane is shown here. Note that the representation is not a unit cell. The green spheres represent Pr while the dark gray are Fe and the turquoise are Al.

Pr-magnetism PrFe$_2$Al$_8$ 15
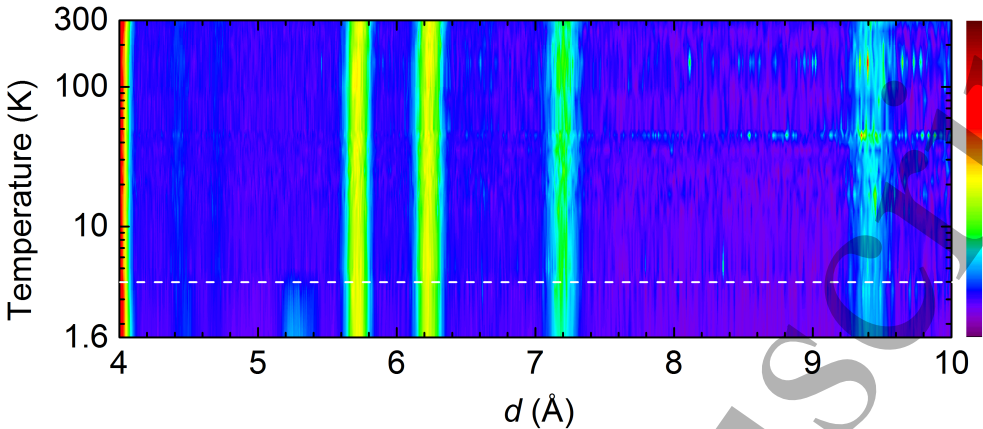

Figure 2. (color online) A colour plot of diffracted intensity from PrFe$_2$Al$_8$ measured at HRPD, plotted as a function of temperature versus d-spacing. The temperature axis is shown in log scale. A horizontal dashed line marks $T_N^{\mathrm{Pr}} \approx 4$ K where the magnetic long-range order of Pr begins as evidenced by the development of intensity at $d \approx$ 5.3 Å.

Pr-magnetism $PrFe_2Al_8$ 16
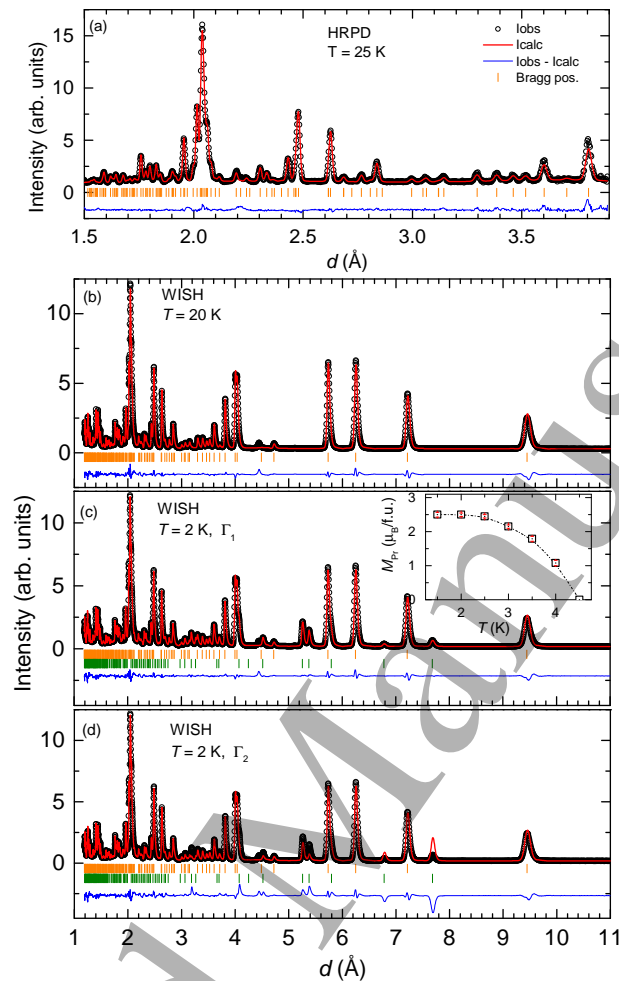
Figure 3. (color online) (a) Neutron powder diffraction intensity of $PrFe_2Al_8$ at 25 K (circles) obtained from the time-of-flight diffractometer HRPD at ISIS facility, UK. Low temperature neutron diffraction pattern of $PrFe_2Al_8$ at (b) 20 K and at (c) 2 K obtained from the diffractometer WISH at ISIS facility, UK. A larger coverage of d-spacing helps in elucidating the magnetic structure of Pr in this compound. In panel (b), the lower set of vertical tick marks correspond to the Bragg peaks of the magnetic structure according to Γ_1 representation. The inset to (c) presents the temperature dependence of refined value of magnetic moment of Pr^{3+} in $PrFe_2Al_8$ showing a phase transition at $T_N^{Pr} = 4.5$ K. (d) The 2 K WISH data refined using the incorrect model Γ_2 does not account for the intensities correctly.

$Pr\text{-}magnetism\ PrFe_2Al_8$ 17
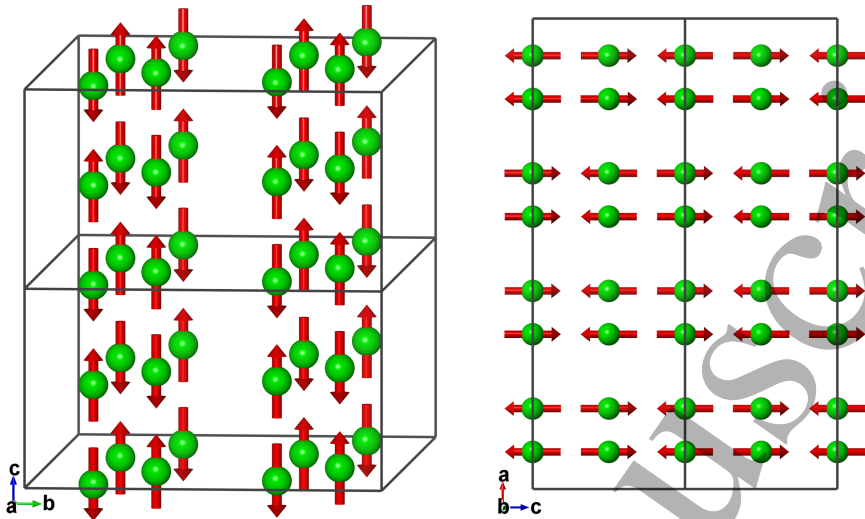
Figure 4. (color online) The magnetic structure of $PrFe_2Al_8$ according to the Γ_1 representation. The Pr^{3+} moments are shown as red arrows ordering antiferromagnetically. Two different views of a $1\times1\times2$ unit cell projected on to the plane are presented.

Pr-magnetism $PrFe_2Al_8$ 18
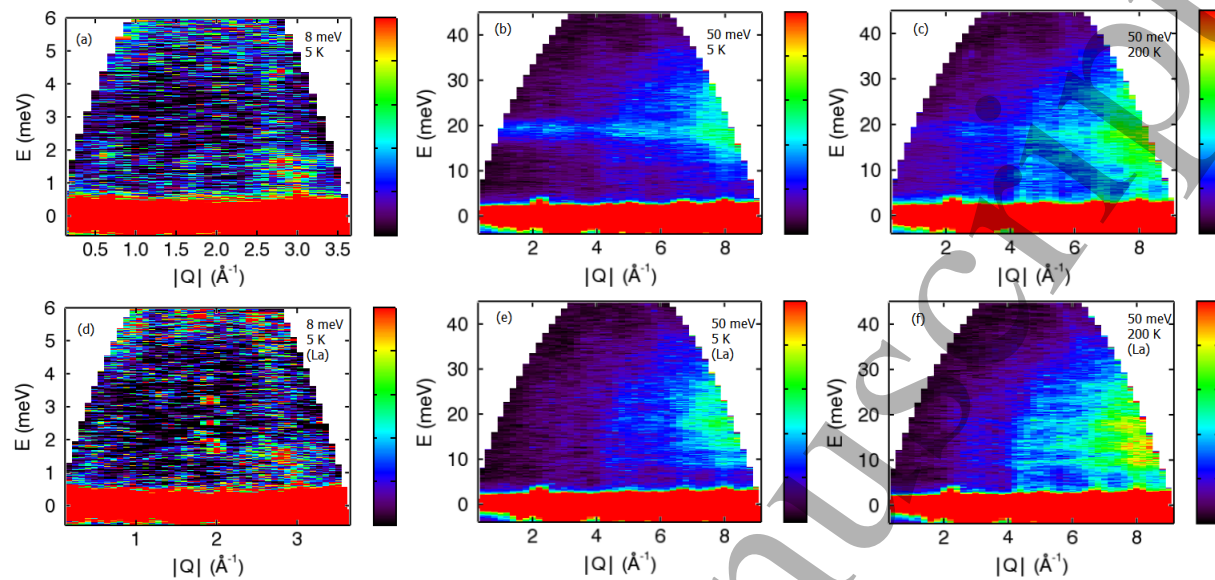
Figure 5. (color online) The color-coded plot of the inelastic neutron scattering intensity of $PrFe_2Al_8$ measured at MARI plotted as energy transfer (E) versus momentum transfer (|Q|) at (a) 5 K, $E_i = 8$ meV (b) 5 K, $E_i = 50$ meV and (c) 200 K, $E_i = 50$ meV; all three for $PrFe_2Al_8$ (d) 5 K, $E_i = 8$ meV (e) 50 K, $E_i = 50$ meV and (f) 200 K, $E_i = 50$ meV for $LaFe_2Al_8$. An inelastic excitation is observed at $E \approx 19$ meV for $PrFe_2Al_8$ (in (b)) which is attributed to crystal field effects. The intensity axes were normalized to a scale of 50 in the units of mbr/sr/meV/fu.

Pr-magnetism PrFe$_2$Al$_8$ 19
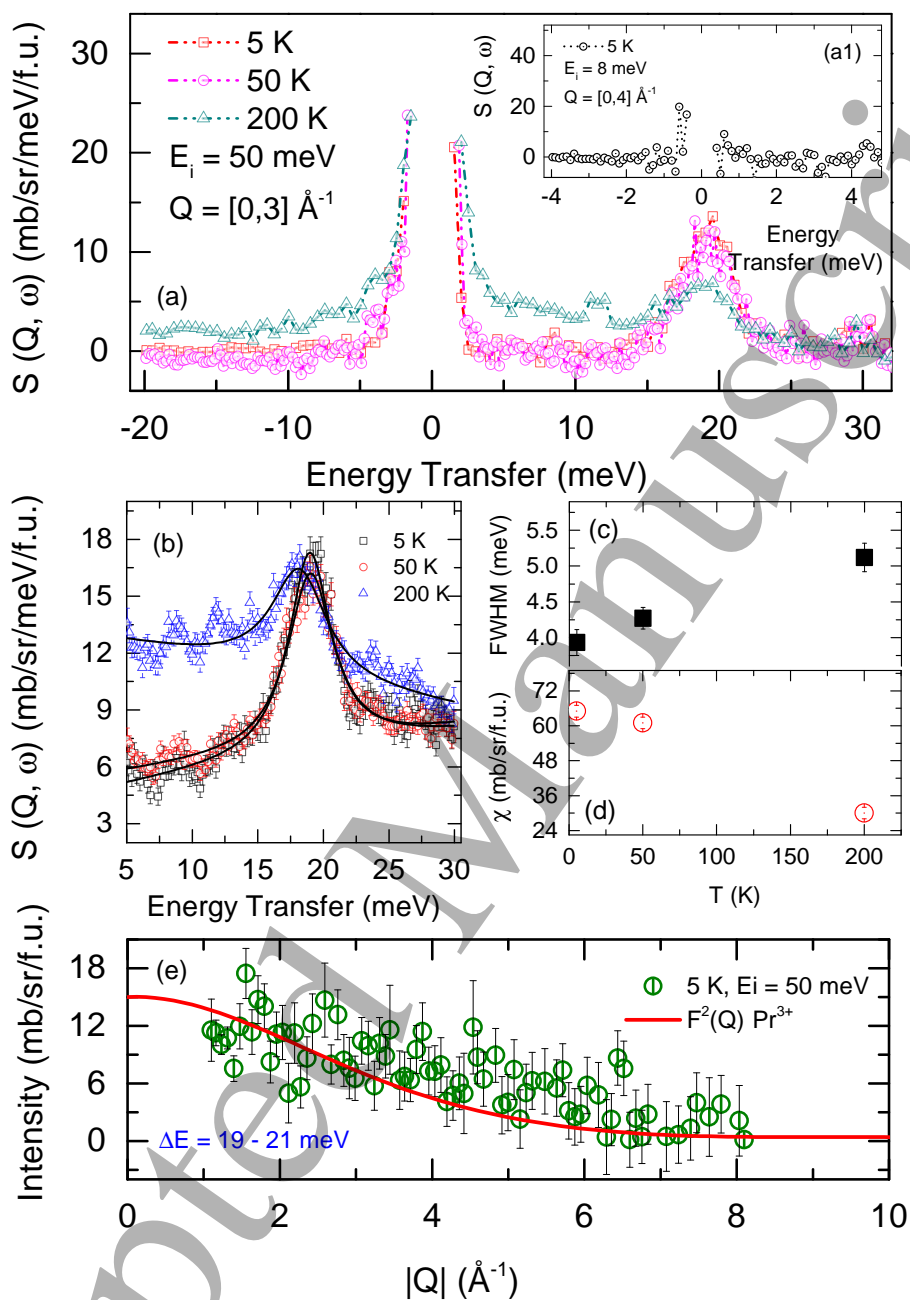
Figure 6. (color online) (a) The dynamic structure factor $S(Q,\omega)$ of PrFe$_2$Al$_8$ at 5 K, 50 K and 200 K plotted as a function of energy transfer ($E_i = 50$ meV). The inset (a1) shows the $S(Q,\omega)$ at 5 K at an incident energy $E_i = 8$ meV where no excitation is observed. The curvefits (black lines), using a Bose-factor modified Lorentzian, to the 19 meV excitation at 5 K, 50 K and 200 K are shown in (b). The temperature dependence of FWHM and the local susceptibility, estimated from the profile fits in (b) are shown in (c) and (d) respectively. In (e) the energy integrated intensity (19 to 21 meV) versus |Q| is plotted along with the magnetic form factor, $F^2(Q)$, for Pr^{3+}. A peak observed near 12 meV in the 200 K data is possibly extrinsic in origin.